Bioresource Technology Reports 33 (2026) 102515

Contents lists available at ScienceDirect

Bioresource Technology Reports

journal homepage: www.sciencedirect.com/journal/bioresource-technology-reports

Short rotation coppice trees in contaminated sites: A study of wood characteristics for bio-concrete applications

Percy Alao [a,*], Edern Philippot [b], Silvia Bibbo [a], Dmitry Tarasov [c], Floran Pierre [d], Jiayun Xu [c], Chunlin Xu [c], Stergios Adamopoulos [a]

[a] Department of Forest Biomaterials and Technology, Swedish University of Agricultural Sciences, Uppsala, Sweden
[b] Institut Technologique FCBA, Domaine Universitaire, 341 rue de la papeterie, 38400, Saint-martin d'Hères, France
[c] Laboratory of Natural Materials Technology, Faculty of Science and Engineering, Åbo Akademi University, Henrikinkatu 2, 20500, Turku, Finland
[d] Vicat, 4, rue Aristide Bergès, 38080, L'Isle d'Abeau, France

ARTICLE INFO

Keywords:
Contaminated-soil wood
Bark
Bio-concrete
Ash content
Chemical composition
pH buffering capacity
Bioremediation

ABSTRACT

Short rotation coppice trees, including poplar (*Populus* spp.), willow (*Salix* spp.), and black locust (*Robinia pseudoacacia* L.), present an exciting opportunity for sustainable biomass production, while also contributing to soil remediation efforts. Harnessing this biomass in construction concrete supports and aligns perfectly with the EU's ambitious 2030 emission targets. Therefore, this study evaluates metal and mineral accumulation and investigates the potential of utilizing wood aggregates as alternative biomass fillers in concrete. Consequently, the cell wall composition, sorption characteristics, metal impurity concentrations, pH, pH buffering capacity, and mineral and ash content of wood and bark obtained from an industrially contaminated site were analysed. The findings reveal that the biomass from the contaminated site had higher mineral content than samples from sawmills. The bark—particularly from black locust—displayed a notable ash content of 8.3 %, largely due to sizeable presence of calcium minerals. In contrast, the wood's ash content was 0.76 %, approximately 1.9 times higher than sawmill wood (0.4 %). Subtle cell wall composition variations were also observed compared to sawmill wood. Overall, the sorption properties, particularly concerning moisture retention, were reflective of lignin content. When evaluating concrete viability, the pH buffering capacity of all examined wood samples was lower, while the bark samples boasted a higher capacity compared to the reference hemp shives. Notably, poplar bark from the contaminated site achieved an average buffering capacity that surpassed the reference bark by 10.9 %. Poplar wood aggregate concretes achieved 0.16 MPa strength and 373 kg/m^3 density, showing optimization potential.

1. Introduction

The environmental impact of the building industry is substantial due to the enormous consumption of natural resources and energy (Lupu et al., 2022). Several studies have highlighted the influence of about 40 % of building construction on total energy consumption in the European Union (EU) (Asdrubali et al., 2015; Olasolo-Alonso et al., 2023; Pérez-Lombard et al., 2008). Thus, the construction industry significantly impacts the environment through greenhouse gas emissions (GHG), excessive energy consumption and depletion of natural resources (Sofiane Amziane, 2016). Cement, a staple in the construction industry, has been identified as a notable environmental polluter (Asghari and Memari, 2024). The implications are that with the continuous rise in the global population, building methods based on the widespread use of high-energy materials such as aluminium, cement, concrete, and steel must be realigned to comply with new directives for the protection of the environment (Morel et al., 2001). The Kyoto Protocol is one of such climate change measures that has led to the EU creating directives in line with the United Nations framework to reduce energy emissions in buildings and limit global temperature rise to below 2 °C while reducing the total emissions of GHG by at least 20 % compared to 1990 levels and by 30 % based on the international agreement (Olasolo-Alonso et al., 2023).

While recent updates show that the EU and its member states reach

* Corresponding author.
E-mail addresses: percy.alao@slu.se (P. Alao), edern.philippot@fcba.Fr (E. Philippot), silvia.bibbo@slu.se (S. Bibbo), dmitry.tarasov@abo.fi (D. Tarasov), floran.pierre@vicat.fr (F. Pierre), jiayun.xu@abo.fi (J. Xu), chunlin.xu@abo.fi (C. Xu), stergios.adamopoulos@slu.se (S. Adamopoulos).

https://doi.org/10.1016/j.biteb.2025.102515
Received 4 August 2025; Received in revised form 20 December 2025; Accepted 25 December 2025
Available online 30 December 2025

their commitments under the Kyoto Protocol's first commitment period (2008–2012), achieving a 19 % reduction in CO_2 gas emissions compared to 1990 levels, the EU has further adopted a set of commission proposals for net greenhouse gas emissions of at least 55 % below 1990 levels by 2030, towards achieving climate neutrality (reductions of 100 %) by 2050 (Commission, 2020). In this regard, the building sector and building materials continue to be critical aspects of focus, considering that zero emissions in buildings, maximised deployment of renewables, and circular economy are identified as one of the seven key enablers to achieve the EU's climate neutrality objectives (Juncker and Cañete, 2018).

Given this, building materials have become indispensable for achieving energy savings in building construction (Abu-Jdayil et al., 2019). This has led to an increased application of natural materials such as wood biomass (sawdust waste), agro-industrial wastes, and plant materials like hemp as alternative materials or additives in building construction (Bakatovich et al., 2022; Lisowski and Glinicki, 2023). Particularly, an eco-friendly bio-aggregate lightweight mixture, which comprises cement, and biomass materials like hemp fibres, wood chips, or agricultural residues, is identified (Lupu et al., 2022). By incorporating these biomass components, the density of the concrete brick reduces and thermal insulating potential increases. This eco-friendly approach leverages the benefits of both cement and biomass to create a construction material that reduce environmental impact while providing thermal insulation. This combination of performance for a building material is particularly valuable for the Northern climate as it fulfils the requirements for viable structures, such as offering thermal insulation and low embodied emissions (Päätalo et al., 2024). Regardless, with such bio-concretes representing a significant step towards sustainable construction, the substantial consumption of natural resources by the building construction sector, exacerbated by global population growth, necessitates further innovation and resource optimization.

As a result, the current research derives from an EU-funded project called FIBSUN (2023–2027). The project aims to promote sustainable fibre production from degraded and marginal European lands to foster resilient and competitive industries and enhance ecosystem services. One primary objective of the project is to investigate wood from contaminated soils to mitigate desertification, organic matter loss, and biodiversity declines in a wide range of soil and CO_2 emissions. For this purpose, fast growing tree species with the ability to tolerate various soil conditions and that offer potential for soil remediation and biomass production are in focus. For resource cycling and sustainable production, this current research then seeks to examine the potential of using contaminant-accumulating, short-rotation tree species, such as poplar (*Populus* spp.) and willow (*Salix* spp.), and black locust (*Robinia pseudoacacia* L.), as prospective wood chips for wood-cement aggregates. These short-rotation trees offer a coppice system with sustainable way to remediate chlor-alkali contaminated sites, while also proving new opportunities for value-added applications, carbon sequestration, and reduction of GHG (Shahariar et al., 2024). The current study comprehensively characterizes the properties of the selected wood species, assesses the extent of absorbed inorganics, and evaluates their suitability for incorporation into concrete formulations. Such thorough characterization of wood and bark from contaminated soil, particularly for bio-concrete applications, has not been well documented. Notably, this research provides a foundational framework for studying around 15 other wood species in consideration for industrial applications within the FIBSUN project.

Hence, the novelty of this research lies in its integrated approach, which combines phytoremediation with the valorisation of bio-based materials. This offers a dual-purpose approach that investigates pollutant absorption by trees while also actively exploring practical applications for the contaminated biomass. Moreover, the research focuses on fast-growing species such as poplar, locust, and willow, making it highly relevant for establishing a sustainable and scalable biomass supply chain. The study also includes a direct comparison to a market standard, hemp shives/hempcrete, and goes beyond simple metal analysis to provide a detailed characterization of the biomass's chemical composition, pH buffering capacity, and other properties. This data is vital for comprehending the material's behaviour and potential interactions within a concrete matrix, thereby providing a clear rationale for incorporating new bio-based resources into sustainable construction.

2. Materials and methods

2.1. Materials

2.1.1. Wood materials

The wood biomasses from poplar (*Populus* spp.), willow (*Salix* spp.), and black locust (*Robinia pseudoacacia* L.) were processed from trees collected from a site with contamination due to previous industrial activities. In the case of black locust, two areas within the sites were focused on, and the wood studied from these areas is termed A1 and A2. The trees were collected on the 6th of February 2024 on former industrial site (Becker Industrial, Le Pont-de-Claix, Grenoble, France), a paint and varnish industry which closed in 2011. The site (depicted in Fig. A.1 in the Supplementary materials) is now operated by Crisalid.

Table 1 presents the diameter and height of harvested trees and the abbreviations for the studied samples. In addition to the harvested tissues, poplar and locust wood from sawmill were examined for comparison. Hemp shives used by Vicat (L'Isle-d'Abeau, France) for the fabrication of hempcretes was also studied as reference material. Examination of the annual rings of the trees at the base showed that all harvested samples were approximately 9 years old. The information about the diameter and height of sawmill-sourced samples is not currently available, and hence the tree age of the wood cannot be identified. The characteristics of the trees were analysed from samples collected from the main trunk. Once the tree had been truncated, the selected trunks were cut into pieces of approximately 60–70 cm long. Of these sections, parts belonging to the tree trunk and main branches was debarked by hand and the debarked logs were shredded. Around 150 g of the unground extracts (full bark samples and wood chips) were used in the characterization. A2's locust shows notable difference in height and diameter than A1's, suggesting more rapid growth for the former. This difference in growth rate may impact the absorption of soil contaminants.

2.1.2. Binder/cement

The binder used is Prompt Natural Cement (PNC). PNC is a natural hydraulic binder, produced from a single raw material: clayey limestone. This limestone, characterized by its fine and consistent

Table 1
Identification of the wood biomass (1 and 2 represent samples from a sawmill and a contaminated site, respectively. (b) represents bark samples).

Nature	Description	Code	Height, m	Diameter, cm
Vicat (V) reference	Hemp shives	VH	–	–
Samples from sawmill (presumed **uncontaminated**) – **1**.	Poplar wood	P1	–	–
	Poplar bark	P1(b)	–	–
	Locust wood	L1	–	–
Samples from **contaminated** site, including black locust harvested from two separate locations (**A1** and **A2**) on the site – **2**.	Poplar wood	P2	4.0	20
	Poplar bark	P2(b)		
	Willow wood (W)	W2	4.2	21
	Willow bark (W(b))	W2 (b)		
	Locust wood ($_{A1}$)	L_{A1}	4.3	13
	Locust bark ($_{A1}$(b))	L_{A1}(b)		
	Locust bark ($_{A2}$(b))	L_{A2}(b)		

composition from homogeneous layers, is fired at temperatures ranging from 500 to 1200 °C. Following firing, the material is crushed and finely ground. PNC's unique composition results in several key characteristics, including rapid setting and hardening, as well as excellent compatibility with plant particles. Manufactured by the Vicat Group (city, France), PNC conforms to French standard NF 15-314 and has been granted European Technical Approval. In selected cases, Portland cement (White CEM1 52,5N, Lafarge Holcim), meeting EN 197-1 standards, was employed as a coating.

2.2. Methods

2.2.1. Soil analysis

Soil samples were collected with a manual auger. A soil sample consists of a composite mixture of at least 5 soil samples homogenized in a bucket. The soil samples were then put in suitable bottles for analyses. Depth of investigation was 0 to 30 cm below surface. The 0–30 cm depth for soil sampling was chosen because this is the recommended level by the Good Practice Guidance for Land Use, Land-Use Change and Forestry (Jim et al., 2003) for the analysis of biodiversity, organics, carbon stocks, and pollutants. Besides, in a case study of a copper mine tailing site (Teng et al., 2022), the soils collected to a depth of 30 cm were found to be the most appropriate for evaluating heavy metal pollution. Similar practices have been used in Australia, where a sampling depth of 30 cm is required to conform with standard accounting procedures. The soil pH, organic carbon, organic matter, water holding capacity (WHC), compactness, apparent density, cation exchange capacity (CEC), and texture were analysed at the CRISALID platform (Grenoble, France). Hydrocarbons (HCT), polycyclic aromatic hydrocarbons (PAHs), polychlorinated biphenyls (PCBs), metalloids, total Kjeldahl nitrogen (TKN), nitrate (NO_3-), and phosphorus were analysed by the Wessling laboratory (Saint-Quentin-Fallavier, France).

2.2.2. Chemical composition and extractive content

Composition of biomass was investigated in two (2) parallels by estimating the content of lipophilic extractives, hemicelluloses, cellulose, acid soluble lignin (ASL), and acid-insoluble lignin (AISL). Lipophilic extractives were removed (Willför et al., 2009) from original biomass material to eliminate its effect on estimation of other biomass components. Lipophilic extractives were isolated in accordance with standard protocol using Soxhlet apparatus and acetone as reaction media. Extractive-free biomass was then lyophilized for 24 h, and the lipophilic extractive content of the original material was determined gravimetrically. The concentration of hemicelluloses, cellulose and lignin was estimated in extractive-free materials. Prior each set of experiments, biomass samples were subjected to lyophilisation.

The composition and concentration of non-cellulosic carbohydrates was determined using acid methanolysis followed by gas chromatography (GC) analysis. It is important to mention that acid methanolysis disintegrates only non-cellulosic polysaccharides and glycosides to monomers, while cellulose units remain unaffected (Willför et al., 2009). The analysis was conducted in accordance with the protocols reported elsewhere (Bertaud et al., 2002; Krogell et al., 2013; Willför et al., 2009). For cellulose content determination, samples were subjected to silylation as described by Krogell et al. (Krogell et al., 2013). Then, glucose content was estimated using GC analysis in accordance with the method suggested by Browning (Browning, 1967) and recently applied in other studies (Krogell et al., 2013).

The total lignin content of plant biomass consists of acid insoluble (AISL or Klason) and acid soluble (ASL) lignin content. Klason lignin was determined gravimetrically in accordance with procedure described by Schwanninger and Hinterstoisser (Schwanninger and Hinterstoisser, 2002). The filtrate collected during the AISL content evaluation was used to determine the ASL content. The concentration of ASL was determined employing UV spectrophotometer (UV-2600, Shimadzu) at absorbance of 205 nm in a cuvette with a 10-nm light path. The 3 % H_2SO_4 solution was employed as a blank and a reference. The ASL content was calculated using the following equations (Eqs. (1) and (2)):

$$B = \frac{A}{110} \times D \tag{1}$$

where B is lignin content in the filtrate in g/L, A is the absorbance, and D is filtrate dilution factor.

$$\text{ASL, wt.\%in wood} = \frac{B \times V \times 100}{1000 \times W} \tag{2}$$

where ASL is acid soluble lignin content, V is total volume of the filtrate, and W is dry weight of wood sample.

2.2.3. Ash content

Ash content was determined using approximately 1 g of each material in five replicates. The samples were dried in an oven at 103 °C for 24 h. The incineration was done using a Gerhardt furnace at 550 °C for about 4 h. The specimens were collected from the furnace after cooling to below 200 °C and were allowed to cool further in a desiccator for about 30 min before weighing. The analysis follows standard practice based on ISO 1171. Ash content was estimated using the equation below:

$$\text{Ash content, \%} = \frac{m_2 - m_o}{m_1} \times 100 \tag{3}$$

where m_o is the mass of the crucible without the sample, m_1 is the mass of the sample in the crucible prior to incineration, and m_2 is the mass of the residue and crucible after incineration.

2.2.4. Thermogravimetric analysis (TGA)

The TGA analysis was done using a Mettler Toledo analyser TGA2 (Mettler Toledo, Greifensee, Switzerland), under a nitrogen atmosphere with a flow rate of 20 mL/min. Samples were milled using a Retsch SM100 mill to pass a 40-mesh screen. Each sample of roughly 6 mg was put in a standard TGA alumina crucible pan. The analysis began with a 5-min isothermal segment at 27 °C, followed by a dynamic heating stage to 600 °C at a rate of 5 °C/min, and concluded with a final 5-min isothermal stage at 600 °C.

2.2.5. Inductively coupled plasma (ICP) analysis

The ICP-MS analysis is an elemental analysis based on SS-EN ISO 17294-2:2016 and SS-EN 14902:2005 standards. The analysis allows for robust identification and quantification of heavy metals and mineral elements with appropriate controls to account for matrix effects and potential interference. The biomass particles <1 mm were pre-cleaned by acid using 2 % HNO_3 to minimize contamination. 0.3 g of each sample was digested with a mixture of 7 mL HNO_3 and 1 mL H_2O_2 under high temperature and pressure in a microwave. The digestion was performed at 200 °C with a power of 1800 W for 20 min. The aliquot of the deionized water (50 mL) diluted sample was analysed with ICP-MS instrument (Thermo Scientific ICP-MS, city, country). An internal standard mixture containing Germanium, Iridium, Rhodium, and Indium was employed to correct for matrix effects. Gold was added to stabilize mercury in solution. The analysis utilized Kinetic Energy Discrimination (KED) mode, employing a collision gas to reduce polyatomic interferences. Some samples, which contained analytes exceeding the calibration curve limits, were further diluted to ensure accurate quantification. In some cases, additional analysis was done with Thermo Scientific iCAP 6300 ICP-OES (optic emission spectroscopy), after decomposition with concentrated nitric acid at 240 °C in Ultra Wave.

2.2.6. Dynamic vapour sorption (DVS) analysis of moisture sorption properties

DVS analysis was performed on the wood dust using a DVS-ET-VID (Surface Measurement Systems (SMS), London, United Kingdom). The samples were oven-dried before the analysis. Both adsorption and

desorption were examined using 20 ± 2 mg of the fine biomass samples with relative humidity (RH) from 10 % to 95 % and temperature of 25 °C at steps of 10 % (RH 10 to 90 %) and 5 % (RH 90 to 95 %).

2.2.7. pH and pH buffering capacity

pH was measured using 1 g of the oven-dried substrates soaked in 20 mL of distilled water and stored at room temperature for 24 h. The measurement was done with four (4) parallels. The pH of the resulting solution was determined using a Metria M21 pH meter. The buffering capacity of the mixture was determined by titration to pH 3 or 10, using two replicates each with 0.05 N HCl or 0.05 N NaOH solutions. This process has been previously applied in past studies (Neitzel et al., 2023; Passialis et al., 2008). However, we highlight the use of HCl rather than Sulfuric acid (H_2SO_4) because the latter is a diprotic acid, meaning each molecule can donate two protons, whereas HCl is monoprotic. The dual dissociation of sulfuric acid adds a layer of complexity and potential error to the titration. In contrast, HCl ensures that every mole of acid added contributes a single, predictable mole of hydrogen protons to the solution, thereby ensuring measurement accuracy.

The buffering capacity ($ƀ_{cap}$) is defined as the number of moles of NaOH (or HCl) required to change the pH of the sample solution by 1 unit. It can also be obtained from the slope of the titration curve. To supplement the analysis of the titration curve, the weighted average buffering capacity ($ƀ_{cap}$) was determined using the buffering capacity in the acidic and basic range, following the equations below:

$$ƀ \text{ in acidic range (initial pH to 3) (or basic (initial pH to 10))} = \frac{\Delta \text{Volume}_{\text{acid (or base)}}}{\Delta \text{pH}_{\text{acid (or base)}}} \times \text{Normality (0.05) of HCl (or NaOH)}$$

Weighted average buffering capacity ($ƀ_{cap}$) is then estimated as shown below:

$$ƀ_{cap} = \frac{ƀ\_\text{acid} \times \Delta\text{pH\_acid} + ƀ\_\text{base} \times \Delta\text{pH\_base}}{(10-3)}$$

where $ƀ_{\_acid}$ and $ƀ_{\_base}$ refer to the buffering capacity in HCl and NaOH; ΔpH_acid and ΔpH_base.

2.2.8. Potential for fabrication of thermal insulation bricks

Preliminary study was conducted based on existing protocol for hempcrete to examine the initial compatibility of the wood and bark as fillers in cement mixture concrete bricks. Most critically, the trial examines the right filler size for the bio-concrete fabrication. In this regard the current work, only examines poplar (P1 and P1(b)) and locust (L1) sourced from the sawmill to achieve necessary data for optimisation that would improve the workability and use of biomass from contaminated soils. Table 2 presents the examined concrete formulation. The quantity of fillers used in base variants A to E was based on their bulk density. Poplar and willow had equivalent densities of 198 kg/m^3 and 200 kg/m^3, respectively. Black locust had the highest density at 237 kg/m^3, while the density of hemp shive was 119 kg/m^3, representing approximately 40 % less than that of poplar. The base amount of cement in the mix was 0.355 kg, i.e. when considering water-cement ratio of 1/1 for A1, B2 and C. Samples A2 and B1 examine lower water fraction with a water/cement (W/C) ratio of 0.76. While C compares the base ratio with lower amounts of biomass aggregates. Samples E1 and E2 are replicates. The chosen modalities should provide valuable data suitable for further experimentation based on the outcome of the biomass filler properties. The selected particle size was such that the variants obtained from mesh with an opening >1 mm but >7 mm was more identical to the reference hemp shive. Therefore, the size of the chips incorporated was within this range. A detailed analysis of the particle size optimisation is planned for a later study.

The biomass fillers in cement aggregates trials were piloted using a cylindrical mould of diameter and height of 11 cm × 22 cm, respectively. The aggregate and about 20 % of the water are first mixed at slow speed for 30 s. Half (1/2) the quantity of cement is added to the mix and blended for 30 s. The remaining quantity of water is then added, and the mix is blended during 1 min. An amount of the blend (1/3) was poured into the cylindrical mould, which was subsequently compressed to 1/3. The first batch was compressed to the target pressure and held for 20 s. Subsequent batches were added and compressed to 2/3 and then 3/3 of the cylinder height, with a 20-s hold after each compression. The material is scraped between each addition to limit the appearance of layers on the final test piece. The samples are removed from the mould after 48 h of setting and then allowed to condition at 20 °C/40 % RH for 28 days. The density (EN 12350-6) and maximum compressive strength (EN 12390-3) of the fabricated samples were measured.

The schematic (Fig. 1) below presents a visual representation of the overall methodology sampling plan and the workflow. The analysis was conducted separately for the wood and bark biomass as highlighted in Table 1. Sawmill samples were also examined, with the wood and bark analysed separately as control samples.

2.2.9. Statistical significance

Average data are reported with standard deviations. If clear differences were not apparent from the mean and deviation, the statistical significance of the results was determined using one-way ANOVA with a 0.05 confidence level. Where significant differences were found, the *p*-value is provided.

3. Results and discussion

3.1. Soil properties

Table 3 details the soil properties. The soil pH values were lower in areas colonized by black locust (A1 and A2), ranging from around 7.3 to 7.8, and higher for poplar and willow soils. A soil pH between 6.0 and 7.5 is generally considered acceptable for most plants and optimal nutrient availability. The pH of the site can be classified as alkaline, which suggests increase likelihood of metal hydroxide precipitation (Sumi et al., 2014). Soil organic carbon and organic matter concentrations in samples from black locust A2 were nearly double those found in samples from black locust A1, as well as in poplar and willow soils. This increased organic content often improves mineral availability due to more microbial activity. Additionally, there is a positive impact on the soil's cation exchange capacity (CEC), which refers to its ability to retain positively charged ions (cations), such as calcium, magnesium, and potassium. The soil sample from black locust A2 exhibited the highest

Table 2
Bio-concrete formulation.

Biomass fillers	P1					P1(b)	L1	
ID	A1	A2	B1	B2	C	D	E1	E2
Grinding disc gap, mm	15	15	5	5	5	5	5	5
Mesh size, mm	>7	>7	3 < x < 7	3 < x < 7	3 < x < 7	3 < x < 7	3 < x < 7	3 < x < 7
Coating	–	–	–		–	Cement (20 %)	–	–
Biomass particles (kg)	0.374	0.374	0.393	0.393	0.278	0.475	0.648	0.648
Water (kg)	0.355	0.270	0.270	0.355	0.355	0.490	0.545	0.545
Water/cement ratio	1.0	0.76	0.76	1.0	1.0	1.38	1.53	1.53

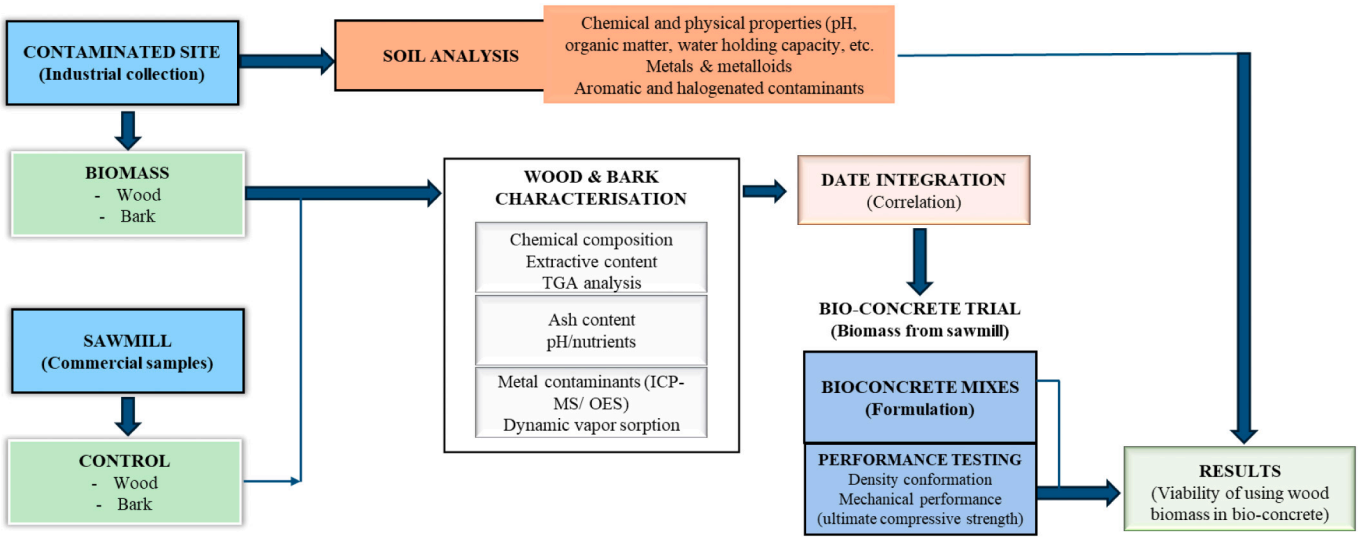

Fig. 1. Sample plan and research workflow.

Table 3
Chemical and physical properties of the soil.

Properties	Parameters	Poplar	Black locust (A1)	Black locust (A2)	Willow
Chemical	pH	8.46	7.37	7.89	8.48
	Organic carbon, %	0.36	0.33	0.67	0.37
	Organic matter	0.62	0.57	1.15	0.65
	Total Kjeldahl Nitrogen (NTK), mg/kg DM	1300	1100	88.9	440
	Nitrate (NO_3^-), mg/kg DM	<100	<100	<100	<100
	Phosphorus (P), mg/kg DM	630	630	1000	530
Physical parameters	WHC[a], mL/100 g of soil	71.43	50	82.52	56.41
	Compactness[b], 0 to 5	1	1	1	0
	Apparent density, g/cm^3	1.41	1.28	1.12	1.16
	CEC, Cmol+/kg	21.50	14.35	34.25	16.30
	Soil texture	Sandy loam	Loam	Sandy loam	Loam

[a] Water holding capacity.
[b] Scale ranging from 0 for very loose soil to 5 for very compact soil.

CEC value at 34.25 cmol+/kg, confirming this correlation. Furthermore, the high organic carbon content improves chelation, thereby enhancing the solubility and availability of micronutrients, including iron (Fe), zinc (Zn), and manganese (Mn), and facilitates their uptake by plant roots (Madhupriyaa et al., 2024).

Other implications of these findings include the binding of the organic matter to heavy metals, which can reduce their bioavailability and uptake by trees. This outcome can have contrasting implications: positive in the case of contaminated soil by reducing the uptake of heavy metals, but potentially detrimental in reducing the uptake of essential micronutrients (Lo et al., 1992). However, black locust A2 soil also exhibited the lowest concentration of total Kjeldahl nitrogen (NTK). Since nitrogen is a critical building block for proteins, enzymes and chlorophyll, such low levels could impact the ability of the tree to cope with environmental stress. Nitrate concentration was the same in all soil samples. However, phosphorus (P) levels were notably higher for black locust (A2) soil. This could have positive implications on soil fertility with potential enhancement of plant nutrient. High phosphorus content reportedly corresponds with increased organic matter inputs into the soil (Department of Primary Industries and Regional Development, 2022).

Overall, the sampled soils were very loose, with an apparent density ranging from 1.123 to 1.413 g/cm^3. The highest soil water holding capacity (WHC) was found for the soil of black locust A2 (82.52 mL/100 g of soil), followed by poplar P1 (71.43 mL/100 g of soil). These two soils had a sandy loam texture. In contrast, black locust A1 and willow soils both had a loam soil texture and corresponding lowest values of CEC and WHC.

In addition to the above observations, only the *Salix* spp. soil sample had no levels of polycyclic aromatic hydrocarbons (PAHs), halogenated hydrocarbons HCTs, and polychlorinated biphenyls (PCBs) or volatile organic compounds and substantially lower concentrations of metals and metalloids compared to the other locations (Table 4). The range of values commonly observed in ordinary soils of all grain sizes in France (Baize, 2000) is also added for reference. The highest levels of PAHs (specifically fluoranthene) and metals/metalloids were observed in the soil with black locust A2, and A1 soil had the most PCB pollution. The

Table 4
Soil composition per site (in mg/kg of soil dry matter).

	Poplar	Black locust (A1)	Black locust (A2)	Willow	France (Baize, 2000)
Hydrocarbon index C10-C40	200	150	120	<20	–
Sum of PAHs	0.59	0.11	0.61	–/–	–
Sum of 7 PCBs	3.7	18	9.5	0.07	–
Chromium (Cr)	100	86	130	22	10 to 90
Nickel (Ni)	28	28	29	25	2 to 60
Copper (Cu)	27	27	46	14	2 to 20
Arsenic (As)	9	7	12	8	1 to 25
Cadmium (Cd)	0.5	0.8	0.9	<0.4	0.05 to 0.45
Mercury (Hg)	0.8	0.2	0.4	<0.1	0.02 to 0.1
Lead (Pb)	360	400	490	20	9 to 50

soil sample for poplar section displayed the highest concentrations of (HCTs) and naphthalene (a type of PAH). Heavy metal contaminant levels were especially lower at the willow location, all falling within the range commonly observed for soils of all grains in France. In contrast, poplar and black locust sites generally exhibited higher heavy metal contaminant levels, except for arsenic (As), and chromium (Cr) in A1, which fall within the range noted for French soils.

3.2. Chemical composition and structural properties

3.2.1. Chemical composition

Fig. 2 highlights the biochemical composition of the samples. The results are indicative as it is difficult to diminutively ascribe the changes in the biochemical composition of the samples to soil contaminants, since other factors such as soil nutrient, precipitation, temperature and light are reportedly crucial (Zhang et al., 2023). Besides, there is currently a lack of information regarding the age of the sawmill samples. However, a study by Donata et al. (2019) indicated that the chemical composition—specifically the cellulose, lignin, and hemicellulose content—of poplar species is not influenced by the species or age of the tree, even for those up to 30 years old. Additionally, the most significant factors affecting extractive content, aside from tree species, are the growth environment. The result in the current study shows that the most obvious implications on composition of the biomass were wood relative to bark. The trend was consistent for all samples with cellulose and hemicelluloses contents being higher in wood than bark. Pectin, lignin and extractive contents were also higher in bark than in wood. These results align with the literature (Safdari et al., 2011), which highlights an increase in lignin (22 to 33 wt%) and a decrease in cellulose (47 to 24 wt%) when comparing poplar bark to wood. This difference is ascribed to the nature of bark cell wall, which is thicker and contains a higher proportion of lignin and other compounds/extractives (tannins, resins, and suberin) essential for its protective function, thus reducing cellulose content. Particularly, suberin, a lipophilic polyester macromolecule, is composed of three building units: long-chain fatty acids (polyaliphatic domain), ferulic acid (polyaromatic domain), and glycerol, which is thought to link these domains. As a structural component, suberin is not easily extracted by common organic solvents. Dou et al. (2021) reported a notable suberin content of 10.7 wt% in black locust bark, potentially explaining the low cellulosic content observed in L_{A1}(b) and L_{A2}(b). The elevated lignin levels in the bark compared to wood and hemp shives (VH) may interfere with the hydration process of cement, potentially slowing down the setting time of the concrete (Carvalho et al., 2023).

Hardwoods, such as poplar, black locust, and willow, typically have a secondary cell wall composition of 35–50 % cellulose, 20–30 % lignin, and 15–25 % hemicelluloses (Isebrands and R., 2014; Murphy et al., 2021). Though, hemicelluloses levels have also been reported to vary between 15 and 35 % (Abik et al., 2023). The results in Fig. 2 are within these values. Hemicelluloses content was in the higher range, from 25 to 29 % and especially utmost in the wood samples from the contaminated site. Large variations in biochemical composition of wood are typical and are due to differences in growth environment (Donata Krutul et al., 2019; Murphy et al., 2021). Poplar sample P2 had slightly lower cellulose (35 ± 1.4 %) than P1 (39 ± 0.7 %), though not significantly (p-value = 0.1). However, P2's extractive content (3.1 ± 0.1 %) was significantly higher (p-value < 0.05) than P1 (2.2 ± 0.0 %). Lignin content was similar between both poplar batches (21–29 wt%), consistent with previous studies (Gao et al., 2022; Sannigrahi et al., 2010). Pectin content was clearly higher in P1(b) (7.2 ± 0.3 wt%) than P2(b) (5.9 ± 0.3 wt%).

Black locust samples showed slight variations in their biochemical content. L1 displayed a higher (p-value < 0.05) lignin content than L_{A1} and L_{A2}, whereas cellulose content was similar (p-value = 0.6) for all. Compared to the other two wood species, black locust often contains lignin in the range of 23–30 wt%. Regardless, the bark samples of black locust presented similar biochemical composition as the poplar variants. However, the levels of ASL were significantly higher in L_{A1}(b) and L_{A2}(b). The high ASL levels could potentially increase water absorption in the cement aggregates, due to its higher proportion of hydrophilic groups (hydroxyl and carboxyl groups). This may cause dimensional instability or cracking in the hardened concrete. While no notable difference existed between the species collected from the site (p-value > 0.05), W2 showed the highest cellulose content (37.2 %).

Among all the wood samples, extractive content was lowest in P1 and W2 (about 2 %). The levels of extractives (5 %) in L1 were notably (p-value < 0.05) higher compared to L_{A1} and L_{A2}, including the bark samples. Unusual soil conditions or possible environmental contamination are potential triggers that might have caused the tree to produce higher levels of extractives as a defence mechanism. Hence, extractives were substantially higher in bark than in the corresponding wood, as typically reported (Gao et al., 2024; Pratyusha, 2022; Uzelac et al., 2023), with W2(b) showing the highest levels at 12.1 %. Fritsch et al. (2022) also noted an extractive content as high as 17 % for *Salix alba*. This substantially high presence of extractives in the harvested willow bark is reportedly due to differences in structural and physiological features, including variations in metabolic pathways, defence strategies, and the presence of a wide range of secondary metabolites, such as salicin and related phenolic compounds, tannins, and flavonoids (Piatczak et al., 2020). High extractive content may potentially cause issues with the adhesion between the biomass and the cement paste,

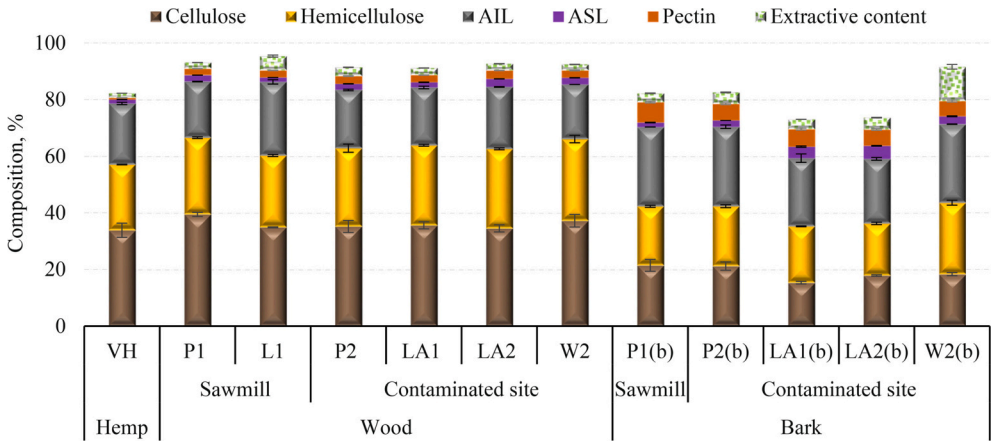

Fig. 2. Cellulose, lignin (AIL, ASL), pectin, hemicellulose, and extractives content of the biomass. VH represents hemp shive; P, L, and W represent Poplar, Locust, and Willow, with 'b' denoting their corresponding bark samples. 1 and 2 represent samples from a sawmill and a contaminated site, respectively. A1 and A2 represent two distinct locations on the contaminated site where locust was sampled.

which could reduce the strength and durability of the product. There may also be potential issues with setting and curing time (Delannoy et al., 2020), dimensional stability, and possible leaching of some extractives over time, which could cause discoloration (Dias et al., 2022).

Poplar (wood and bark) from the contaminated site had significantly (p-value > 0.05) higher extractives than sawmill poplar. While sawmill black locust's wood also shows high extractive content raising makes regarding site implications. In the context of bio-concrete application, the effect of high extractive content in wood biomass can be quite complex, offering both positive and negative effects depending on the type and concentration of the extractives (Gao et al., 2024). In addition to the issues earlier noted, extractive levels can cause variability and inconsistencies in the properties of the concrete (Karade, 2016). Conversely, moderate levels could improve water repellence, adhesion enhancement in some cases and reduction of alkali-aggregate reactions that can weaken concrete over time. Regardless, the use of bark in concrete-mix should be explored due to improved workability (Jong-Chan Kim et al., 2020), low density and sustainability from lowering the environmental impact of concrete production (Giannotas et al., 2022).

3.2.2. Ash content and minerals

The ash content of the biomass, which primarily reflects the amount of absorbed minerals like calcium (Ca), potassium (K), and magnesium (Mg), varied across samples (see Figs. B.1 and B.2 in the Supplementary materials). While a positive correlation between ash and mineral content was generally observed, some minerals may volatilize during incineration, influencing the final ash levels. This was particularly evident when comparing the hemp shive (VH) reference sample to the non-bark substrates of willow and locust. Despite VH's high overall mineral content, its low ash content (0–1 %) was not significantly different from the other samples ($p = 0.32$). This outcome is typically because ash is the residue left after burning organic materials, and it primarily consists of the minerals contained in the tissues. However, though they are closely related, some minerals or inorganic compounds can volatize during incineration (Wang et al., 2025). Therefore, the lower ash content of VH despite its high mineral content is predominantly due to K, which forms more volatile compounds during combustion than calcium (the primary mineral in the wood samples).

P1 exhibited a notably lower ash content (p-value $= 0.003$), while P2's ash content was significantly higher than VH's (p-value $= 0.037$). It is generally reported that hemp shives exhibit lower ash content compared to hardwoods (Angelini et al., 2014). Among wood samples from the contaminated site, P2 showed significantly higher mineral and ash content than L_{A2} and W2 (p-value $= 0.03$), while L_{A1} was similar to P2 (p-value $= 0.05$). Locust bark had significantly higher mineral accumulation than poplar and willow bark, which showed similar levels (p-value $= 0.5$). It is important to note that, despite the high cation exchange capacity (CEC) of the contaminated soil from site A2 (Table 3), Ca was the only mineral that was significantly higher in sample L_{A2}(b) compared to sample L_{A1}(b). In contrast, K and Mg levels were higher in L_{A1}(b). This difference can be explained by a phenomenon known as growth dilution, where a plant's rapid growth rate leads to a decrease in the concentration of minerals within its tissues. The enhanced growth is evident in the diameter and width of the locust from site A2, which were greater than those of the locust tree from site A1 (Table 1). While poplar bark from the sawmill (P1(b)) contained about 22.5 % more Ca than its counterpart from contaminated site (P2(b)), their ash content was not significantly different ($p = 0.4$). This is attributed to the fact that P2(b) had significantly higher levels of other minerals (K, Mg, Mn, P), which were approximately twice those of P1(b). Furthermore, the overall mineral and ash content of poplar wood from the sawmill (P1) was significantly lower than that of P2, as P2 contained 1.5 times more calcium and 5.5 times more K. L1's higher mineral content and comparable ash content to L_{A1}/L_{A2} (p-value $= 0.1$), supports K volatility during combustion.

The specific content of wood and bark can be different, depending on tree age, species, and growth environment (Komán, 2018). Although the study by Passialis et al. (2008) reported that ash content decreased by almost two- to threefold in wood from older trees compared to younger trees, the results in the current study suggest a negligible age difference between the sawmill and contaminated-soil samples. This holds true particularly when comparing poplar bark from the sawmill to the bark variant from the contaminated site, and locust wood from the sawmill to the batches from the contaminated soil. Alternatively, the results could indicate that the samples from the contaminated site exhibit a high mineral and ash content, despite their relatively young age of approximately nine years. This is also supported by Donata et al. (2019), who found no notable differences in the mineral content of 7-year-old wood compared to much older batches of 30 years.

The implications of high minerals or ash content as it concerns wood additives in concrete mixtures can potentially lead to cement hydration, causing a reduction in the compressive and flexural strength of the concrete (Gao et al., 2024). However, certain benefits exist with moderate contents, such as enhancement of durability by better resistance to weathering, frost damage, and chemical attack while the presence of high calcium and magnesium oxides can be beneficial for fire resistance. This likely indicates that the use of wood and bark as fillers in the cement aggregate might be detrimental. The barkless wood samples from the contaminated site, might offer more advantages in this regard.

3.2.3. Thermogravimetric analysis

Fig. 3 illustrates the mass loss (ML) and weight derivative (DTGA) curves of the samples. Asides the initial thermal decomposition of moisture and volatile solubles at temperatures below 125 °C, significant weight loss was observed between 200 and 300 °C and can be primarily attributed to the decomposition of hemicelluloses. The precise temperature range for this process varied among the samples, reflecting differences in the types and structures of hemicelluloses present. Lignin typically degrades over a broad temperature range, approximately 160–900 °C, while the most pronounced peak in the DTGA curve, occurring around 300–400 °C, corresponds to the degradation of cellulose. Notable differences in thermal behaviour were also observed, with additional decomposition peaks around 150 °C and approximately 500 °C in the bark samples. The peak at 150 °C signifies the decomposition of extractives in bark. Typically, thermal decomposition or phase transition of mineral compounds occurs at elevated temperatures. Specifically, minerals like calcium (Ca) and magnesium (Mg) can decompose to form metal oxides and carbon dioxide gas. Consequently, the peak observed at approximately 500 °C suggests a higher concentration of Ca and Mg in the bark samples, which is as noted in Section 3.2.2. In the case of sample L_{A1}(b), an additional decomposition peak around 200 °C was evident, which likely corresponds to the breakdown of specific extractives present in L_{A1}(b) but not found in the other bark samples. Hemp shives exhibited thermal behaviour similar to wood samples. However, the sharper decomposition peak and lower residual mass in hemp shives suggest a more homogeneous composition and a lower mineral content.

Thermal decomposition analysis with temperatures (T_5, T_{10}, and T_{50}) at 5 %, 10 % and 50 % ML, respectively (Table 5), confirms the variations in the chemical composition of the samples, particularly regarding lignin, cellulose, hemicelluloses, and extractives. The lower T_5 for bark samples was reportedly due to the presence of more thermally unstable components, such as fatty acids and volatile extractives that undergo rapid volatilization when heated (Mészáros et al., 2004). This result aligns with the chemical composition analysis. The degradation pattern of L_{A1}(b) was distinct with additional peaks observed at about 210 °C. Despite having the highest T_{50} (380 °C), L_{A2}(b) showed a lower T_5 (196 °C), confirming an initial loss of labile components followed by a thermally stable residue. This discrepancy signifies differences in the composition of extractives, potentially including terpenoids and low-molecular-weight phenolics, such as eugenol and guaiacol, as noted in earlier studies of similar biomass (Martinez-Gil et al., 2020). This

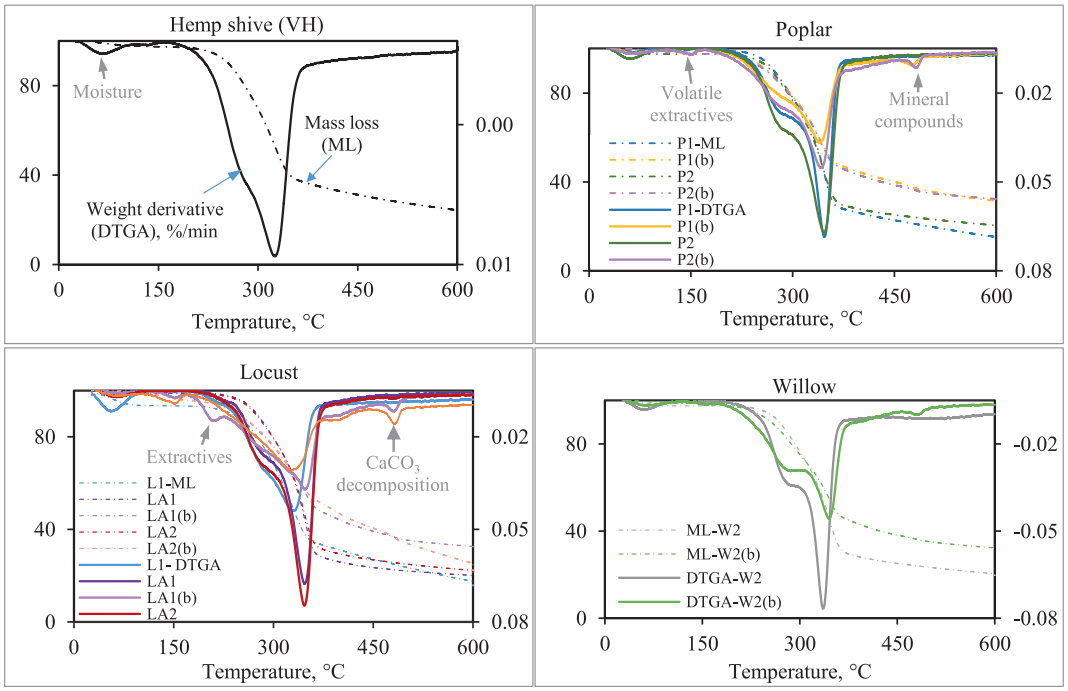

Fig. 3. TGA curves: Mass loss (ML) curve is represented by a dashed line, while the derivative thermogravimetric analysis (DTGA) curve is shown with a solid line (as depicted in VH). The numbers 1 and 2 denote samples from a sawmill and a contaminated site, respectively. A1 and A2 represent two distinct locations on the contaminated site where locust was sampled.

Table 5
TGA residue and thermal decomposition temperatures corresponding to 5 %, 10 % and 50 % ML.

Biomass	Source	Sample ID	T_5, °C	T_{10}, °C	T_{50}, °C	Residues, %
Hemp shives	Vicat	VH	231.7	259.3	333.6	23.3
Wood	Sawmill	P1	256.3	272.6	341.5	13.6
		L1	238.0	264.3	355.8	15.4
	Contaminated site	P2	245.8	268.5	340.8	19.7
		L_{A1}	256.3	274.6	342.3	19.6
		L_{A2}	212.3	272.6	344.0	21.6
		W2	255.4	271.6	343.2	20.4
Corresponding bark	Sawmill	P1(b)	235.5	263.3	357.8	30.3
	Contaminated site	P2(b)	230.4	261.1	354.9	31.8
		L_{A1}(b)	212.3	246.2	361.0	32.0
		L_{A2}(b)	196.0	245.7	380.1	22.2
		W2(b)	227.9	256.2	353.6	31.8

observation might explain the lower residue observed with L_{A1}(b) compared to other bark samples. Black locust bark typically contains a range of extractives, including tannins, flavonoids, and robinin (Hong et al., 2021), with flavonoids known for their role in stress response (Chen et al., 2023). P1 demonstrated the lowest residue level at 13.6 %, indicating a reduced non-volatile content. Despite the high levels of extractives in W2(b), the decomposition pattern was quite similar to the other bark samples and more closely related to black locust bark. Bark's

Table 6
Mean values or measured content of heavy metals in the biomass samples with deviations (in bracket).

Biomass samples		ID	Micrograms of the metal per gram of total solid (TS), mg/kg						
			Copper (Cu)	Cadmium (Cd)	Arsenic (As)	Nickel (Ni)	Zink (Zn)	Lead (Pb)	Iron (Fe)
Hemp	Shives	VH	$3.4^{(0.1)}$	<0.1	–	–	$4.9^{(0.2)}$	$1.7^{(0.1)}$	$46.9^{(1.7)}$
Wood	Poplar	P1	$1.5^{(0.1)}$	$0.43^{(0.01)}$	$0.02^{(-)}$	<0.5	$11.6^{(0.6)}$	$16.7^{(0.6)}$	$6.0^{(0.3)}$
		P2	$3.1^{(0.8)}$	$0.31^{(0.05)}$	$0.06^{(-)}$	<0.5	$20.6^{(2.9)}$	$8.1^{(7.7)}$	$9.2^{(0.1)}$
	Locust	L1	$1.9^{(0.1)}$	$0.14^{(0.10)}$	$0.04^{(-)}$	<0.5	$4.3^{(0.3)}$	$10.4^{(13.5)}$	$16.2^{(0.4)}$
		L_{A1}	$3.1^{(1.1)}$	$0.17^{(0.05)}$	$0.03^{(-)}$	<0.3	$5.1^{(1.3)}$	$33.8^{(1.1)}$	$13.7^{(1.9)}$
		L_{A2}	$3.5^{(0.8)}$	$0.15^{(0.09)}$	$0.04^{(-)}$	<0.5	$4.3^{(0.7)}$	$45.0^{(22)}$	$21.0^{(1.9)}$
	Willow	W2	$3.0^{(0.4)}$	$0.31^{(0.01)}$	$0.03^{(-)}$	<0.3	$26.6^{(0.6)}$	$38.9^{(13.5)}$	$9.6^{(0.5)}$
Bark	Poplar	P1(b)	$4.2^{(0.2)}$	$0.44^{(0.02)}$	$0.14^{(-)}$	<0.5	$89.0^{(4.4)}$	$36.6^{(9.9)}$	$105.8^{(8.8)}$
		P2(b)	$5.6^{(0.2)}$	$0.33^{(0.00)}$	$0.07^{(-)}$	$1.1^{(0.1)}$	$158^{(6.9)}$	$50.5^{(6.0)}$	$48.0^{(0.4)}$
	Locust	L_{A1}(b)	$4.5^{(0.4)}$	$0.74^{(0.01)}$	$0.05^{(-)}$	<0.3	$184^{(3.2)}$	$22.0^{(2.5)}$	$39.8^{(0.5)}$
		L_{A2}(b)	$6.1^{(0.4)}$	$0.14^{(0.11)}$	$0.04^{(-)}$	$1.1^{(0.2)}$	$11.6^{(0.4)}$	$21.2^{(2.7)}$	$59.0^{(1.7)}$
	Willow	W2(b)	$4.7^{(0.04)}$	$0.72^{(0.04)}$	$0.04^{(-)}$	0.6	$156^{(4.9)}$	$53.1^{(8.2)}$	$32.7^{(4.7)}$

higher T_{50} than wood results from slower decomposition due to lignin, stable extractives, minerals, and complex interactions between the major components in bark.

3.3. Accumulation of heavy metals

3.3.1. ICP

Table 6 highlights the heavy metal contents in the samples. Zinc (Zn) was present in significant amounts, particularly in bark. Zn is a necessary mineral for plant growth and development and is regarded as one of the highly absorbed micronutrients, including Mn and Cu (Hamzah Saleem et al., 2022; Ledin, 1996). Hence, it is readily absorbed and stored by the tissues. However, a notable observation was the very low levels of Zn in L_{A2}(b). It is most likely that the proximity of the location (A1) to the main road might have impacted Zn intake. While soil proximity to the road could account for increased levels of micronutrients, such as Zn, due to the deposition of Zn particles from tire wear (Councell et al., 2004), an indirect effect with negative impact on nutrient uptake mechanisms may suffice due to high levels of air pollutions from traffics (Muthu et al., 2021). Comparing the locust woods, there was no difference in Zn levels among L1, L_{A1}, and L_{A2}. Cu content was significantly (p-value < 0.05) high for samples collected from the site relative to those from the sawmill. Compared to VH, there was no meaningful difference in Cu levels relative to the wood samples from the site. Locust wood from site A2 showed the highest Cu levels, which correlates with observed concentrations in the soil. Despite the low measure of heavy metal components for the willow site (see Table 4), the levels of heavy metal absorption were somewhat comparable and, in some cases, even higher than black locust and poplar samples. This outcome is likely due to wood species variation factors, like those mentioned by Tozser et al. (2023). A fast growth rate in the case of locust from site A2, may have caused a decrease in metal concentrations by reducing the quantity of stored metals in the wood (Lovynska et al., 2023). A similar observation was highlighted with the comparison of absorbed minerals between the locust samples. Moreover, the outcome for the black locust samples reflects the already known fact about the tolerance and exclusion ability of the species. When comparing wood and bark intakes, a noteworthy distinction was the high levels of Pb in black locust wood (L_{A1} and L_{A2}) than bark, though the variation within the wood was substantially higher. Typically, tree bark is a sink for deposition and accumulation of materials absorbed from the soil. Hence, bark is commonly used as a bioindicator of pollution because its structure and porosity contribute to the longer preservation of pollutants compared to other parts of the tree (Zoltan Pásztory et al., 2016).

Overall, heavy metal content was higher in the biomass obtained from the Grenoble site than sawmill samples, except for Pb in P1. P2's high heavy metal levels, alongside mineral volatility, may explain ash/mineral discrepancies. P1(b) had high Fe; P2(b) also showed elevated Fe. Poplar sawmill samples had higher Cd compared to the harvested samples, but L_{A1}(b) and W2(b) showed the highest overall levels of Cd. A study conducted by Ledin (1996) on *Salix alba* showed that the measured levels of Ni (0.5 μg/g) and Cu (13 mg/kg) for willow harvested from a conventional forest are notably higher compared to the results of the current study. However, the comparatively low amounts of Pb (1.1 mg/kg) and, particularly, Cd (<0.15 mg/kg) raise a cause for concern. In another study (Lovynska et al., 2023), the Pb concentrations in black locust ranged from 0.53 mg/kg to 1.56 mg/kg across different sites, while Cd concentrations varied from 0.004 mg/kg to 0.029 mg/kg. These concentrations are relatively low, even compared to the sample batch from the sawmill. The elemental composition of the wood biomass, in general, differs from VH, showing lower levels of Cd, Pb, and Zn, but a higher level of Fe, especially in comparison to wood without bark.

3.4. Properties of the wood biomass for concrete application

3.4.1. pH and pH buffering capacity

Wood samples, including bark, exhibited a pH range of 4.1 to 4.5, notably more acidic than VH at 5.7 (see Fig. C.1 in the Supplementary materials). Within wood samples, only black locust (L_{A1} and L_{A2}) showed statistically significant higher acidity (p-value < 0.05) compared to their corresponding bark samples (L_{A1}(b) and L_{A2}(b)). Although bark is generally thought to be more acidic than wood due to higher concentrations of acidic extractives, this study did not universally support that trend. This difference may arise from the complex interplay of several factors, including the specific composition of extractives, growing conditions, and mineral content. For instance, the elevated lignin content in bark (as discussed in Section 3.2.1) is expected to enhance acidity because of the presence of phenolic hydroxyl and carboxylic acid groups (Liu et al., 2018). This effect was observed regarding the differences in pH of VH compared to the wood biomass. However, the higher ash content/mineral measured in the bark samples impacted the pH towards a more alkaline level. Ultimately, the impact of lignin on acidity in the bark appears to have been overshadowed by the neutralizing effect of the compounds of these minerals.

Regarding site implications, P1(b) and P2(b) had identical pH values of 4.5, and the pH difference between P1 and P2 was not statistically significant (p-value $= 0.168$), although P2 was slightly less acidic. For black locust, L1 has a substantially lower acidity than both L_{A1} and L_{A2} (p-value $= 0.014$ and 0.0013, respectively). This outcome correlates with the higher mineral content in L1.

The pH buffering capacity is essential characteristic because of the highly alkaline environment of PNC upon hydration. Therefore, a high buffering capacity is necessary to maintain the high pH during the initial setting and hardening of the PNC. Furthermore, a stable pH contributes to a more predictable and controlled setting time for the PNC concrete. The titration curve of the biomass samples is presented in the Supplementary materials (Fig. C.2). The region where the curve is flatter, and a low steepness of slope indicates where the change in pH with the addition of titrant is minimal. In other words, a flatter and less steep slope suggests higher buffering capacity. Hence, VH appeared to display a higher buffering capacity compared to all the wood samples without bark. However, bark samples showed higher buffering capacity than VH and their relative wood samples. Black locust bark, particularly L_{A1}(b) and L_{A2}(b), stood out as having the highest capacity to buffer against increases in pH. P2(b) and P1(b) showed similar levels of buffering capacity while the P1 had a slightly higher buffering capacity compared to P2.

Buffering capacity is a non-linear property and, as such, cannot be simply summed across the acidic and alkaline pH ranges. Instead, the weighted average buffering capacity $ƀ_{cap}$, derived from the buffering capacities in acidic and basic pH ranges, serves as a comprehensive metric that summarizes the overall behaviour of the material. The slope of the titration curve at specific points indicates the buffering capacity within those respective pH ranges, which are distinct characteristics. Thus, the limitation yet is that while the weighted average provides a general overview, it overlooks local details. However, these details were previously captured by the titration curve and by evaluating the range of pH vis-à-vis buffering capacity in Fig. 4, a comprehensive result is achieved. Fig. 4 shows that VH exhibited notably higher buffering capacity in both acidic (0.087 mol/L·pH) and basic (0.057 mol/L·pH) ranges, with a $ƀ_{cap}$ of (0.07 mol/L·pH) than non-bark wood samples. While bark samples largely showed higher buffering capacity than wood, L_{A1}(b) achieved the highest $ƀ_{cap}$ (0.12 mol/L·pH), with a $ƀ_{\_base}$ of 0.099 mol/L·pH, and L_{A1} has the lowest $ƀ_{cap}$ (0.03 mol/L·pH) and $ƀ_{\_base}$ (0.025 mol/L·pH). This trend of bark having greater buffering capacity than wood aligns with previous studies (Xiaodong Wang et al., 2010). And conforms to higher mineral and phenolic compounds found in bark, which contain numerous hydroxyl (—OH) groups (Tanase et al., 2019).

The P1 and P2 samples exhibited similar pH buffering capacities.

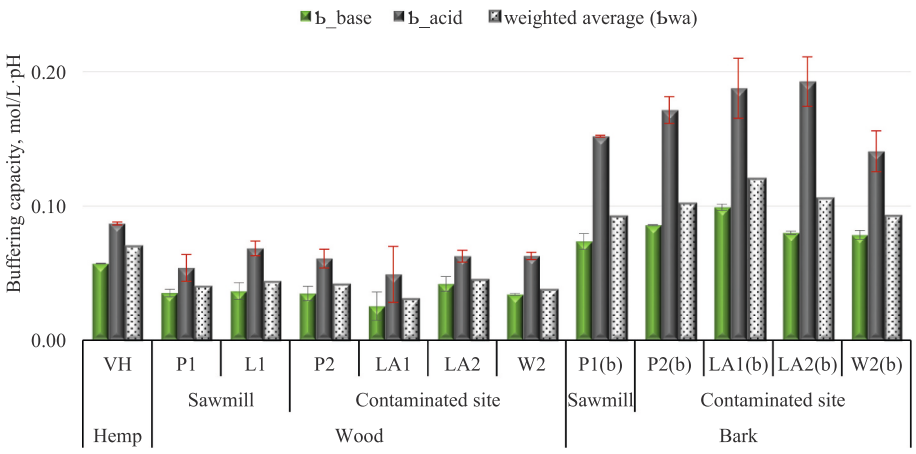

Fig. 4. Comparison of the estimated pH buffering capacity across biomass samples. The figure shows buffering capacity in basic media (b_base), acidic media (b_acid), and the weighted average (bwa). Samples are grouped by biomass type (hemp, wood, and bark (b)) and source (sawmill (1) and contaminated site (2)).

However, P2(b) demonstrated a higher buffering capacity than P1(b). These variations in buffering capacity correlate with observed differences in heavy metal contaminants. The overall trend, excluding L_{A1}, indicates that samples from the examined site show a greater buffering capacity than commercially sourced samples. The low buffering capacity of L_{A1} may be due to low mineral and extractive contents coupled with the impact of soil pH levels (7.38). Soil pH plays a crucial role in the easy formation of metal hydroxides in wood. Alkaline pH tends to decrease metal solubility in wood. In the case of L_{A2}(b), the high buffering capacity suggests that the ratio of metals in the samples is a critical factor rather than their absolute concentrations. For example, even though L_{A2}(b) has lowest levels of some measured metal contaminants (Pb, and Zn) compared to other bark samples from the Grenoble site, the levels of Cu, Ni and Fe are highest, as highlighted in Table 6. These metals can form hydroxides, particularly under slightly alkaline conditions, which can contribute to enhanced buffering capacity in addition to the effects of the high mineral content.

The higher $ƀ_{cap}$ observed in samples from contaminated soil, particularly from bark, suggests potential benefits for compatibility with PNC in concrete applications by helping to maintain a more stable and optimal pH during the initial stages of PNC setting and hardening. However, as shown by sample L_{A1}, there is significant variability in properties among the samples, which poses a challenge for achieving consistent and predictable performance in concrete.

3.4.2. Moisture sorption (DVS)

Fig. 5 illustrates the moisture sorption behaviour of the biomass samples alongside that of the reference hemp (VH). A major factor impacting sorption of lignocellulosic materials is the availability of accessible hydroxyl groups (—OH) within cell walls. This —OH availability is largely influenced by the chemical composition and physical structure of the material (Thybring et al., 2017). It has been identified that the abundance of —OH in cellulose and hemicelluloses presents more hygroscopicity compared to lignin (Heise et al., 2022). Additionally, factors such as crystallinity (in cellulose) and the degree of cross-linking (in lignin) affect —OH accessibility (Park et al., 2010). Aside from P2, VH displayed a higher equilibrium moisture content (EMC) than wood samples, mostly at elevated relative humidity (RH) levels. Considering the similarities in cellulose composition between VH and the wood samples, and despite VH containing lower levels of hemicelluloses, the higher hygroscopic nature of VH compared to the wood samples indicate a higher degree of amorphous cellulose in VH. Furthermore, low levels of extractives were earlier highlighted for VH in Fig. 2. This shows that fewer hydrophobic compounds are blocking access to —OH groups. Nevertheless, poplar bark samples presented a similar EMC to VH, while L_{A1}(b) even surpassed it. Bark samples consistently show a higher EMC than the corresponding wood samples, due to more amorphous components in bark. When comparing wood samples based on their origin, though not so obvious, P2 generally had a slightly higher EMC than P1. This highlights the parallels with the observed variations in the chemical composition, such as the 12 % higher cellulose content of P1 and the 18 % more pectin in P2. At 0 % RH, P2 retained 1.6 % moisture than P1 (0.51 %), despite only a 1.5 % lignin difference. P2's higher extractives and inorganics likely explain this. Bark samples showed a similar trend: P2(b)'s retention was 13.5 % higher than P1(b). Black locust bark (L_{A1}(b), L_{A2}(b)) exhibits substantially higher EMC than wood (L_{A1}, L_{A2}) at nearly all RH values. At 95 % RH, bark EMC ranged 20–26 % and wood 19–21 %. L1's elevated EMC, probably due to higher extractives, contrasts sharply with L_{A1}/L_{A2}. Minor site-specific variations were observed, but sawmill vs. Grenoble differences was pronounced. Black locust wood water retention aligns with lignin content. L1's higher lignin (27.5 %) likely explains its increased moisture retention (0.66 %) versus L_{A1}/L_{A2}. However, small moisture differences suggest that extractives also influenced retention. W2(b) displays higher EMC than W2, similar to poplar and black locust.

Overall, the magnitude of moisture behaviour difference is comparable across wood species. P2's sorption is closest to VH, with W2 being intermediate. Contamination subtly shifted poplar's sorption towards VH. Bark enhanced sorption across species, aligning them with VH. Contaminated poplar's sorption similarity to VH indicates its potential as VH alternative.

3.4.3. Properties of the wood biomass-cement aggregate samples

Fig. 6(a) shows images of the fabricated concrete cylindrical samples, demonstrating the feasibility of adapting the Vicat hempcrete protocol for the wood-cement concrete. Fig. 6(b) presents the maximum ultimate compressive strength and density of the wood-concrete samples. Compared to the hemp reference sample, all the bio-concrete with wood fillers showed higher densities but lower compressive strengths. Samples A1 (338 kg/m^3) and A2 (328 kg/m^3) achieved a density close to the hempcrete (300 kg/m^3). Regardless of aggregate size, excluding the C concrete mix, a trend of increasing density with increasing wood filler content was observed. However, the water-to-cement ratio (w/c) appears to be a significant factor affecting ultimate compressive strength. At a w/c of 0.76, using a wood fraction of B1 (0.393 kg) compared to A2 (0.374 kg), resulted in an 8.8 % increase in density and a 25 % increase in compressive strength. Increasing the w/c to 1 resulted in a 50 % increase in ultimate compressive strength for the A-concrete batches and a 60 % increase for the B-concrete variants. This improved performance with a higher water-cement ratio is attributed to increased water availability for the cement hydration, leading to more of the primary binding phase in concrete.

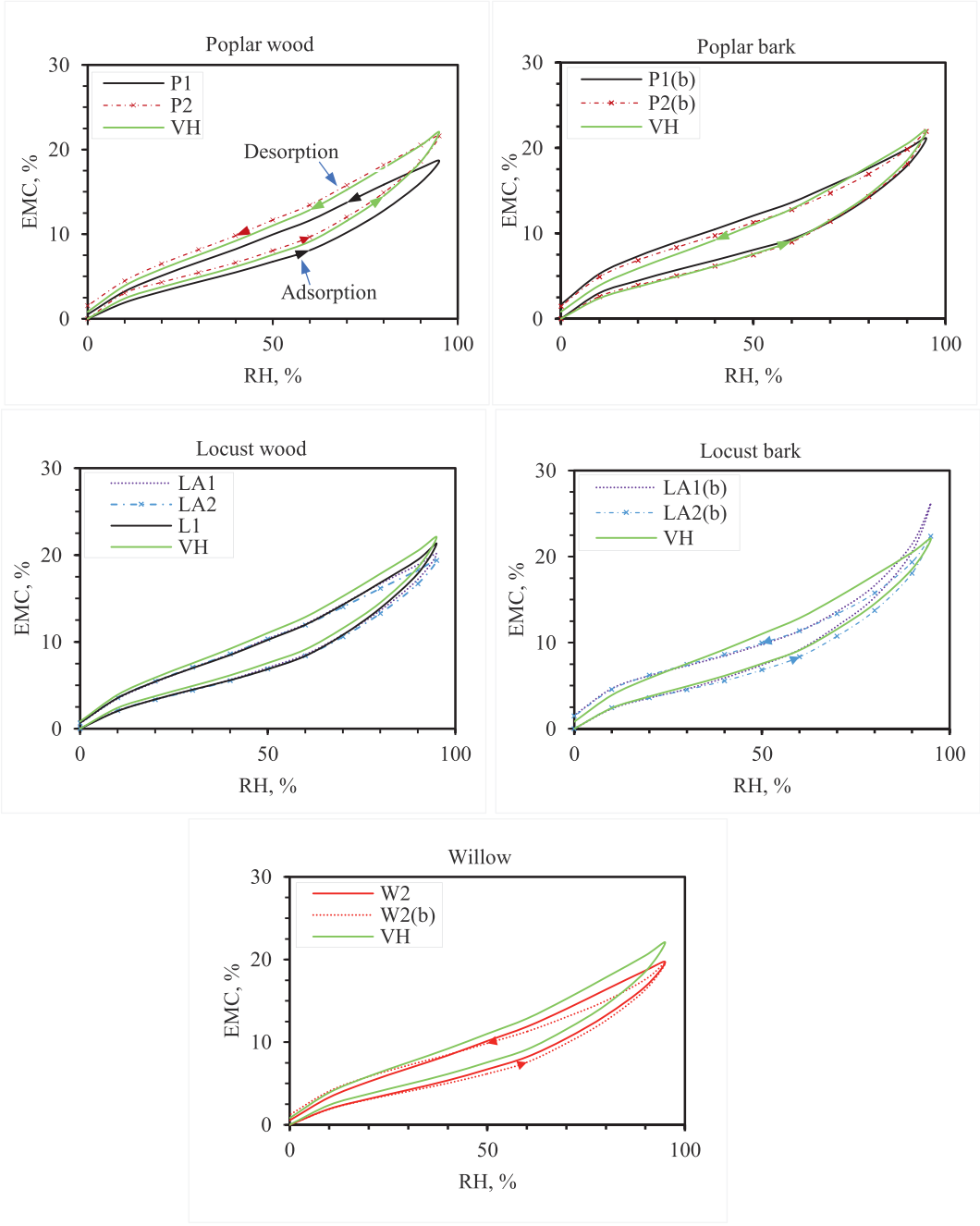

Fig. 5. Dynamic vapour sorption hysteresis of wood and bark biomass from the sawmill and contaminated site, compared to Vicat hemp (VH).

Compared to sample A1, B2 displayed a 7 % increase in density and a 33 % increase in ultimate compressive strength. This slight decrease in density, combined with the significant improvement in strength relative to the differences in w/c, suggests enhanced hydration. Smaller aggregate sizes appear to be more effective in achieving higher compressive strength due to several factors, including a larger surface area, which promotes stronger interfacial bonding with the cement paste (Poon et al., 2004). Additionally, studies on concrete porosity confirm that a higher proportion of smaller particles reduces void content and directly correlates with increased density and compressive strength (Rakesh Kumar, 2002). However, the quantity of smaller wood particles used in B2 to achieve a comparable bulk density with the reference VH led to a higher overall density, indicating that further optimization is needed. When comparing the A and B batch concretes at a w/c of 1 with batch C, which had lower biomass loading, the densities and compressive strengths of C and B2 were comparable, and both were higher than A1. This is likely due to the differences in aggregate size, as evidenced by the improved ultimate compressive strength observed with smaller biomass particles blended using w/c of 0.76. Consequently, the higher density arises from a more compact structure achievable with smaller particles. While the density similarities between C and B2 are noteworthy, further investigation is necessary. For reference, in France, the hemp construction guideline recommends a maximum compressive strength of 0.2 MPa for a density of approximately 300 kg/m^3.

Results, especially with 5 mm disc gap, indicate higher filler loading does not reliably improve bio-concrete performance. Biomass characteristics, such as species differences, also likely impacted results. Furthermore, particles exceeding 7 mm may hinder product quality. Bark extractives/minerals, along with its fraction and w/c ratio, likely influenced bark-filled concrete (D) relative to the C, A1 and B2.

(a)

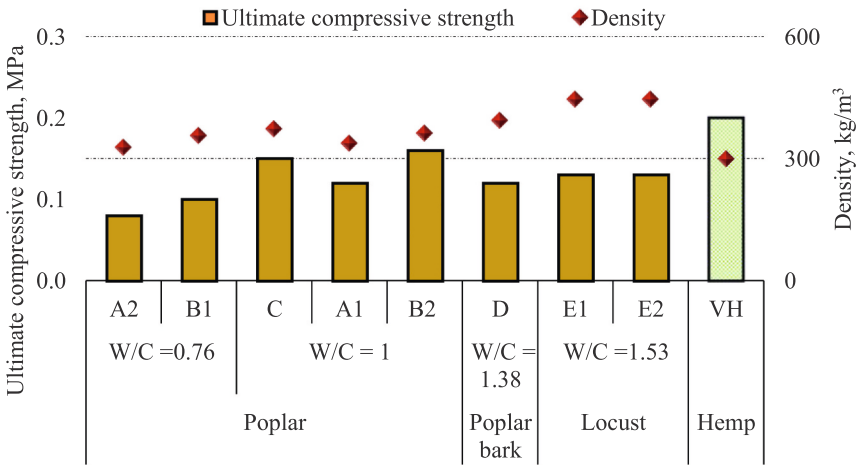

(b)

Fig. 6. (a) Sample image of fabricated biomass filled-concrete blocks and (b) Ultimate compressive strength and density of bio-concrete mixes. The figure compares the ultimate compressive strength (bar chart, left axis) and density (red diamond markers, right axis) of samples. The mixes are made from poplar wood, poplar bark, locust wood, and hemp shives (VH), with the water-cement ratio (W/C) also indicated. (For interpretation of the references to colour in this figure legend, the reader is referred to the web version of this article.)

Nonetheless, D-concrete shows promise versus A2 and B1 (w/c 0.76). While the biomass-concretes did not meet hempcrete targets, these trials are encouraging. With refined w/c and quality control, desired biomass-filled concrete can attainable.

4. Conclusions

This study successfully investigated the potential of using wood and bark from poplar, willow, and locust trees harvested from a contaminated industrial site in Grenoble, France, as an alternative to traditional bio-fillers like hemp shives for cement aggregate bricks. The research provides a comprehensive characterization of these fast-growing tree species, offering critical insights into their properties and a viable pathway for their valorisation.

The analysis of metal contaminants revealed significant levels of lead (Pb) and cadmium (Cd), with black locust wood showing a notable ability to accumulate Pb. Bark consistently exhibited higher levels of lignin, extractives, and mineral content than wood, which correlated with higher ash content and pH buffering capacity. This mineral presence, dominated by calcium (Ca) and potassium (K), was a key factor influencing the material's properties. Poplar samples particularly demonstrated a balanced profile of minerals and contaminants that positioned them as the most suitable candidates for further application.

This research successfully developed and tested a wood-cement composite using poplar chips. The resulting samples achieved a density of 363 kg/m^3, comparable to the 300 kg/m^3 density of hempcrete, indicating a strong potential for these materials in the construction sector.

This study contributes to a more sustainable construction industry by presenting a new method for processing contaminated biomass into a valuable resource. We established a comprehensive dataset that highlights the potential of specific tree species, while providing a solid foundation for future research focused on optimizing biomass-cement applications. This research transforms what was once regarded as waste into a promising new material for the circular economy.

CRediT authorship contribution statement

Percy Alao: Writing – review & editing, Writing – original draft, Validation, Supervision, Investigation, Formal analysis. **Edern Philippot:** Writing – review & editing, Writing – original draft, Investigation, Funding acquisition, Formal analysis. **Silvia Bibbo:** Writing – original draft, Investigation. **Dmitry Tarasov:** Writing – review & editing, Validation, Funding acquisition. **Floran Pierre:** Writing – review & editing, Investigation, Funding acquisition. **Jiayun Xu:** Investigation, Funding acquisition. **Chunlin Xu:** Supervision, Funding acquisition, Conceptualization. **Stergios Adamopoulos:** Writing – review & editing, Supervision, Funding acquisition, Conceptualization.

Institutional review board statement

Not applicable.

Submission declaration and verification

Authors declare that the work described has not been published previously, is not under consideration for publication elsewhere, and that the publication is approved by all authors and tacitly or explicitly by

the responsible authorities where the work was carried out, and that, if accepted, it will not be published elsewhere in the same form, in English or in any other language, including electronically without the written consent of the copyright-holder.

All authors have read and agreed to the published version of the manuscript.

Declaration of Generative AI and AI-assisted technologies in the writing process

Authors declare the use of artificial intelligence (AI) in improving grammar in the writing process. During the preparation of this work the author(s) used [Gemini (Google)] to [search for applicable literature and improve spelling and grammatical structure]. Grammarly AI was also used for grammatical checks to improve writing. After using these tools, the author(s) reviewed and edited the content as needed and take(s) full responsibility for the content of the publication.

Funding

The work was supported by the Circular Bio-based Europe Joint Undertaking and its members and funded under the European Union Horizon-JU-CBE Project: 101112318, FIBSUN - Novel fibre value chains and ecosystem services from sustainable feed stocks (2023–2027).

Declaration of competing interest

The authors declare that they have no known competing financial interests or personal relationships that could have appeared to influence the work reported in this paper.

Acknowledgement

Jiayun Xu would like to acknowledge the BioDemo – Demonstrating the Value Chains of a New Field of Industry project co-funded by European Regional Development Fund and Helsinki-Uusimaa Regional Council.

Edern Philippot would like to acknowledge Envisol, a company specialised in consulting and engineering offering services in the field of polluted sites and soils, for their soil analysis and characterization work at the Pont-de-Claix site in France and especially to acknowledge the work of Maxime Louzon, Marie Colette and Thomas Curie.

Appendix A. Supplementary data

Supplementary data to this article can be found online at https://doi.org/10.1016/j.biteb.2025.102515.

Data availability

Data will be made available on request.

References

Abik, F., Palasingh, C., Bhattarai, M., Leivers, S., Strom, A., Westereng, B., Mikkonen, K. S., Nypelo, T., 2023. Potential of wood hemicelluloses and their derivates as food ingredients. J. Agric. Food Chem. 71 (6), 2667–2683. https://doi.org/10.1021/acs.jafc.2c06449.

Abu-Jdayil, B., Mourad, A.-H., Hittini, W., Hassan, M., Hameedi, S., 2019. Traditional, state-of-the-art and renewable thermal building insulation materials: an overview. Constr. Build. Mater. 214, 709–735. https://doi.org/10.1016/j.conbuildmat.2019.04.102.

Angelini, L.G., Tavarini, S., Cestone, B., Beni, C., 2014. Variation in mineral composition in three different plant organs of five fibre hemp (*Cannabis sativa* L.) cultivars. Agrochimica 58 (1).

Asdrubali, F., D'Alessandro, F., Schiavoni, S., 2015. A review of unconventional sustainable building insulation materials. Sustain. Mater. Technol. 4, 1–17. https://doi.org/10.1016/j.susmat.2015.05.002.

Asghari, N., Memari, A.M., 2024. State of the art review of attributes and mechanical properties of hempcrete. Biomass 4 (1), 65–91. https://doi.org/10.3390/biomass4010004.

Baize, D., 2000. Teneurs totales en « métaux lourds » dans les sols français. In: Courrier de l'environnement de l'INRA, vol. 39, pp. 39–54.

Bakatovich, A., Gaspar, F., Boltrushevich, N., 2022. Thermal insulation material based on reed and straw fibres bonded with sodium silicate and rosin. Constr. Build. Mater. 352. https://doi.org/10.1016/j.conbuildmat.2022.129055.

Bertaud, F., S., A., Holmbom, B., 2002. Evaluation of acid methanolysis for analysis of wood hemicelluloses and pectins. Carbohydr. Polym. 48, 319–324.

Browning, B.L., 1967. Methods of Wood Chemistry. John Wiley & Sons, New York.

Carvalho, V.R., Costa, L.C.B., Baeta, B.E.L., Peixoto, R.A.F., 2023. Lignin-based admixtures: a scientometric analysis and qualitative discussion applied to cement-based composites. Polymers (Basel) 15 (5). https://doi.org/10.3390/polym15051254.

Chen, S., Wang, X., Cheng, Y., Gao, H., Chen, X., 2023. A review of classification, biosynthesis, biological activities and potential applications of flavonoids. Molecules 28 (13). https://doi.org/10.3390/molecules28134982.

Commission, E, 2020. Communication From the Commission to the European Parliament, the Council, the European Economic and Social Committee and the Committee of the Regions Stepping Up Europe's 2030 Climate Ambition Investing in a Climate-neutral Future for the Benefit of Our People.

Councell, T.B., Duckenfield, K.U., Landa, E.R., Callender, E., 2004. Tire-wear particles as a source of zinc to the environment. Environ. Sci. Technol. 38 (15). https://doi.org/10.1021/es034631f.

Delannoy, G., Marceau, S., Glé, P., Gourlay, E., Guéguen-Minerbe, M., Diafi, D., Amziane, S., Farcas, F., 2020. Impact of hemp shiv extractives on hydration of Portland cement. Constr. Build. Mater. 244. https://doi.org/10.1016/j.conbuildmat.2020.118300.

Department of Primary Industries and Regional Development, G.o.W.A, 2022. Soil Organic Matter Influence on Nutrient Availability, vol. 2025 (Australia).

Dias, S., Almeida, J., Santos, B., Humbert, P., Tadeu, A., António, J., de Brito, J., Pinhão, P., 2022. Lightweight cement composites containing end-of-life treated wood – leaching, hydration and mechanical tests. Constr. Build. Mater. 317. https://doi.org/10.1016/j.conbuildmat.2021.125931.

Donata Krutul, A.A., Radomski, Andrzej, Drożdżek, Michał, Kłosińska, Teresa, Zawadzki, Janusz, 2019. The chemical composition of poplar wood in relation to the species and age of trees. For. Wood Technol. 105, 125–132.

Donata, K., Andrzej, A., Andrzej, R., Michał, D., Teresa, K., Janusz, Z., 2019. The chemical composition of poplar wood in relation to the species and the age of trees. Ann. WULS For. Wood Technol. 131–138. https://doi.org/10.5604/01.3001.0013.7642.

Dou, J., Evtuguin, D.V., Vuorinen, T., 2021. Structural elucidation of suberin from the bark of cultivated willow (*Salix* sp.). J. Agric. Food Chem. 69 (37), 10848–10855. https://doi.org/10.1021/acs.jafc.1c04112.

Fritsch, C., Dumarçay, S., Colin, F., Gérardin, P., 2022. Bark composition changes along the trunk of three softwood species: *Picea abies*, *Abies alba* Mill. and *Pseudotsuga menziesii*. Scand. J. For. Res. 37 (5–8), 314–319. https://doi.org/10.1080/02827581.2022.2132283.

Gao, W., Zhou, L., Liu, S., Guan, Y., Gao, H., Hui, B., 2022. Machine learning prediction of lignin content in poplar with Raman spectroscopy. Bioresour. Technol. 348, 126812. https://doi.org/10.1016/j.biortech.2022.126812.

Gao, C., Cui, X., Matsumura, J., 2024. Multidimensional exploration of wood extractives: a review of compositional analysis, decay resistance, light stability, and staining applications. Forests 15 (10). https://doi.org/10.3390/f15101782.

Giannotas, G., Kamperidou, V., Stefanidou, M., Kampragkou, P., Liapis, A., Barboutis, I., 2022. Utilization of tree-bark in cement pastes. J. Build. Eng. 57. https://doi.org/10.1016/j.jobe.2022.104913.

Hamzah Saleem, M., Usman, K., Rizwan, M., Al Jabri, H., Alsafran, M., 2022. Functions and strategies for enhancing zinc availability in plants for sustainable agriculture. Front. Plant Sci. 13, 1033092. https://doi.org/10.3389/fpls.2022.1033092.

Heise, K., Koso, T., King, A.W.T., Nypelo, T., Penttila, P., Tardy, B.L., Beaumont, M., 2022. Spatioselective surface chemistry for the production of functional and chemically anisotropic nanocellulose colloids. J. Mater. Chem. A Mater. 10 (44), 23413–23432. https://doi.org/10.1039/d2ta05277f.

Hong, G., Chen, Z., Han, X., Zhou, L., Pang, F., Wu, R., Shen, Y., He, X., Hong, Z., Li, Z., He, W., Wei, Q., 2021. A novel RANKL-targeted flavonoid glycoside prevents osteoporosis through inhibiting NFATc1 and reactive oxygen species. Clin. Transl. Med. 11 (5), e392. https://doi.org/10.1002/ctm2.392.

Isebrands, J.G., R., J., 2014. Poplars and Willows: Trees for Society and the Environment. The Food and Agriculture Organization of the United Nations and CABI, Rome, Italy.

Jim, P., Michael, G., Taka, H., Thelma, K., Dina, K., Riitta, P., Leandro, B., Kyoko, M., Todd, N., Kiyoto, T., Fabian, W., 2003. Good Practice Guidance for Land Use, Land-use Change and Forestry.

Jong-Chan Kim, J.-H.C., Kim, Jong-Hwa, Cho, Seong-Min, Park, Sang-Woo, Cho, Young-Min, Park, Se-Yeong, Kwak, Hyo Won, Choi, In-Gyu, 2020. Development of lignin-based polycarboxylates as a plasticizer for cement paste via peracetic acid oxidation. Bioresources 15 (4), 8133–8145. https://doi.org/10.15376/biores.15.4.8133-8145.

Juncker, J.-C., Cañete, M.A., 2018. Going Climate-neutral by 2050, Special Eurobarometer on Climate Change, September 2017. Publications Office of the European Union, Luxembourg, p. 2019.

Karade, S., 2016. Developments in Cement-bonded Composite Material Technology. National Seminar on Modern Trends in Architectural and Civil Engg. Practices, Roorkee, pp. 57–64.

Komán, S., 2018. Energy-related characteristics of poplars and black locust. BioResources 13 (2), 4323–4331.

Krogell, J., Korotkova, E., Eränen, K., Pranovich, A., Salmi, T., Murzin, D., et al., 2013. Intensification of hemicellulose hot-water extraction from spruce wood in a batch extractor - effects of wood particle size. Bioresour. Technol. 143, 212–220.

Ledin, S., 1996. Willow wood properties, production and economy. Biomass Bioenergy 11 (2–3), 75–83. https://doi.org/10.1016/0961-9534(96)00022-0.

Lisowski, P., Glinicki, M.A., 2023. Promising biomass waste–derived insulation materials for application in construction and buildings. Biomass Convers. Biorefinery. https://doi.org/10.1007/s13399-023-05192-8.

Liu, Q., Luo, L., Zheng, L., 2018. Lignins: biosynthesis and biological functions in plants. Int. J. Mol. Sci. 19 (2). https://doi.org/10.3390/ijms19020335.

Lo, K.S.L., Yang, W.F., Lin, Y.C., 1992. Effects of organic matter on the specific adsorption of heavy metals by soil. Toxicol. Environ. Chem. 34 (2–4), 139–153. https://doi.org/10.1080/02772249209357787.

Lovynska, V., Holoborodko, K., Ivanko, I., Sytnyk, S., Zhukov, O., Loza, I., Wiche, O., Heilmeier, H., 2023. Heavy metal accumulation by *Acer platanoides* and *Robinia pseudoacacia* in an industrial city (Northern Steppe of Ukraine). Biosyst. Divers. 31 (2), 246–253. https://doi.org/10.15421/012327.

Lupu, M.L., I., D.N., Baciu, I.-R., Maxineasa, S.G., Pruna, L., Gheorghiu, R., 2022. Hempcrete - modern solutions for green buildings. In: 16th International Scientific Conference: Civil Engineering and Building Services (CIBv 2021) Online. IOP Publishing Ltd.

Madhupriyaa, D., Baskar, M., Sherene Jenita Rajammal, T., Kuppusamy, S., Rathika, S., Umamaheswari, T., Sriramachandrasekran, M.V., Mohanapragash, A.G., 2024. Efficacy of chelated micronutrients in plant nutrition. Commun. Soil Sci. Plant Anal. 55 (22), 3609–3637. https://doi.org/10.1080/00103624.2024.2397019.

Martinez-Gil, A., Del Alamo-Sanza, M., Sanchez-Gomez, R., Nevares, I., 2020. Alternative woods in enology: characterization of tannin and low molecular weight phenol compounds with respect to traditional oak woods. A review. Molecules 25 (6). https://doi.org/10.3390/molecules25061474.

Mészáros, E., Jakab, E., Várhegyi, G., Szepesváry, P., Marosvölgyi, B., 2004. Comparative study of the thermal behavior of wood and bark of young shoots obtained from an energy plantation. J. Anal. Appl. Pyrolysis 72 (2), 317–328. https://doi.org/10.1016/j.jaap.2004.07.009.

Morel, J.C., Mesbah, A., Oggero, M., Walker, P., 2001. Building houses with local materials: means to drastically reduce the environmental impact of construction. Build. Environ. 36 (10), 1119–1126. https://doi.org/10.1016/s0360-1323(00)00054-8.

Murphy, E.K., Mottiar, Y., Soolanayakanahally, R.Y., Mansfield, S.D., 2021. Variations in cell wall traits impact saccharification potential of *Salix famelica* and *Salix eriocephala*. Biomass Bioenergy 148. https://doi.org/10.1016/j.biombioe.2021.106051.

Muthu, M., Gopal, J., Kim, D.-H., Sivanesan, I., 2021. Reviewing the impact of vehicular pollution on road-side plants—future perspectives. Sustainability 13 (9). https://doi.org/10.3390/su13095114.

Neitzel, N., Eder, M., Hosseinpourpia, R., Walther, T., Adamopoulos, S., 2023. Chemical composition, particle geometry, and micro-mechanical strength of barley husks, oat husks, and wheat bran as alternative raw materials for particleboards. Mater. Today Commun. 36. https://doi.org/10.1016/j.mtcomm.2023.106602.

Olasolo-Alonso, P., López-Ochoa, L.M., Las-Heras-Casas, J., López-González, L.M., 2023. Energy performance of buildings directive implementation in Southern European countries: a review. Energ. Buildings 281. https://doi.org/10.1016/j.enbuild.2022.112751.

Päätalo, J., Alao, P.F., Rohumaa, A., Kers, J., Liblik, J., Lylykangas, K., 2024. Prefab light clay-timber elements for net zero whole-life carbon buildings. J. Sustain. Archit. Civ. Eng. 34 (1), 89–100. https://doi.org/10.5755/j01.sace.34.1.35561.

Park, S., Baker, J.O., Himmel, M.E., Parilla, P.A., Johnson, D.K., 2010. Cellulose crystallinity index: measurement techniques and their impact on interpreting cellulase performance. Biotechnol. Biofuels 3, 10. https://doi.org/10.1186/1754-6834-3-10.

Passialis, C., Voulgaridis, E., Adamopoulos, S., Matsouka, M., 2008. Extractives, acidity, buffering capacity, ash and inorganic elements of black locust wood and bark of different clones and origin. Holz Roh Werkst. 66 (6), 395–400. https://doi.org/10.1007/s00107-008-0254-4.

Pérez-Lombard, L., Ortiz, J., Pout, C., 2008. A review on buildings energy consumption information. Energ. Buildings 40 (3), 394–398. https://doi.org/10.1016/j.enbuild.2007.03.007.

Piatczak, E., Dybowska, M., Pluciennik, E., Kosla, K., Kolniak-Ostek, J., Kalinowska-Lis, U., 2020. Identification and accumulation of phenolic compounds in the leaves and bark of *Salix alba* (L.) and their biological potential. Biomolecules 10 (10). https://doi.org/10.3390/biom10101391.

Poon, C.S., Shui, Z.H., Lam, L., 2004. Effect of microstructure of ITZ on compressive strength of concrete prepared with recycled aggregates. Constr. Build. Mater. 18 (6), 461–468. https://doi.org/10.1016/j.conbuildmat.2004.03.005.

Pratyusha, S., 2022. Phenolic Compounds in the Plant Development and Defense: An Overview. IntechOpen, Rijeka.

Rakesh Kumar, B.B., 2002. Porosity, pore size distribution and in situ strength of concrete. Cem. Concr. Res. 33 (1), 155–164. https://doi.org/10.1016/S0008-8846(02)00942-0.

Safdari, V., Khodadadi, H., Hosseinihashemi, S.K., Ganjian, E., 2011. The effects of poplar bark and wood content on the mechanical properties of wood-polypropylene composites. BioResources 6 (4), 5180–5192. https://doi.org/10.15376/biores.6.4.5180-5192.

Sannigrahi, P., Ragauskas, A.J., Tuskan, G.A., 2010. Poplar as a feedstock for biofuels: a review of compositional characteristics. Biofuels Bioprod. Biorefin. 4 (2), 209–226. https://doi.org/10.1002/bbb.206.

Schwanninger, M., Hinterstoisser, B., 2002. Klason lignin: modifications to improve the precision of the standardized determination. Holzforschung 56 (2), 161–166. https://doi.org/10.1515/HF.2002.027.

Shahariar, S., Soolanayakanahally, R., Bedard-Haughn, A., 2024. Short rotation willow to restore degraded marginal land and enhance climate resiliency within the Prairie Pothole Region: a potential nature-based solution. Nat.-Based Solut. 5. https://doi.org/10.1016/j.nbsj.2024.100129.

Sofiane Amziane, M.S., 2016. Overview on bio-based building material made with plant aggregate. In: RILEM Technical Letters, vol. 1, pp. 31–38. https://doi.org/10.21809/rilemtechlett.2016.9.

Sumi, H., Kunito, T., Ishikawa, Y., Nagaoka, K., Toda, H., Aikawa, Y., 2014. Effects of adding alkaline material on the heavy metal chemical fractions in soil under flooded and non-flooded conditions. Soil Sediment Contam. Int. J. 23 (8), 899–916. https://doi.org/10.1080/15320383.2014.890169.

Tanase, C., Cosarca, S., Muntean, D.L., 2019. A critical review of phenolic compounds extracted from the bark of woody vascular plants and their potential biological activity. Molecules 24 (6). https://doi.org/10.3390/molecules24061182.

Teng, Y., Liu, L., Zheng, N., Liu, H., Wu, L., Yue, W., 2022. Application of different indices for soil heavy metal pollution risk assessment comparison and uncertainty: a case study of a copper mine tailing site. Minerals 12 (9). https://doi.org/10.3390/min12091074.

Thybring, E.E., Thygesen, L.G., Burgert, I., 2017. Hydroxyl accessibility in wood cell walls as affected by drying and re-wetting procedures. Cellulose 24 (6), 2375–2384. https://doi.org/10.1007/s10570-017-1278-x.

Tozser, D., Horvath, R., Simon, E., Magura, T., 2023. Heavy metal uptake by plant parts of *Populus* species: a meta-analysis. Environ. Sci. Pollut. Res. Int. 30 (26), 69416–69430. https://doi.org/10.1007/s11356-023-27244-2.

Uzelac, M., Sladonja, B., Sola, I., Dudas, S., Bilic, J., Famuyide, I.M., McGaw, L.J., Eloff, J.N., Mikulic-Petkovsek, M., Poljuha, D., 2023. Invasive alien species as a potential source of phytopharmaceuticals: phenolic composition and antimicrobial and cytotoxic activity of *Robinia pseudoacacia* L. leaf and flower extracts. Plants (Basel) 12 (14). https://doi.org/10.3390/plants12142715.

Wang, Y., Chen, W., Chen, Y., Zhang, S., Deng, B., 2025. Volatilization and retention of metallic and non-metallic elements during thermal treatment of fly ash. Materials 18 (6). https://doi.org/10.3390/ma18061319.

Willför, S., Ali, M., Karonen, M., Reunanen, M., Arfan, M., Harlamow, R., 2009. Extractives in bark of different conifer species growing in Pakistan. hfsg 63 (5), 551–558. https://doi.org/10.1515/hf.2009.095.

Xiaodong Wang, Z.H., Cooper, Paul, Wang, Xiang-Ming, Zhang, Yaolin, Casilla, Romulo, 2010. The ability of wood to buffer highly acidic and alkaline adhesives. Wood Fiber Sci. 42 (3).

Zhang, B., Liu, G., Feng, Z., Zhang, M., Ma, T., Zhao, X., Su, Z., Zhang, X., 2023. Constructing a model of *Poplus* spp. growth rate based on the model fusion and analysis of its growth rate differences and distribution characteristics under different classes of environmental indicators. Forests 14 (10). https://doi.org/10.3390/f14102073.

Zoltan Pásztory, I.R.M., Gorbacheva, Galina, Börcsök, Zoltán, 2016. The utilization of tree bark. BioResources 11 (3), 7859–7888.